

DETERMINING THE MULTI-CURRENT SOURCES OF  
MAGNETOENCEPHALOGRAPHY BY USING FUZZY  
TOPOGRAPHIC TOPOLOGICAL MAPPING

WAN ENY ZARINA WAN ABDUL RAHMAN

UNIVERSITI TEKNOLOGI MALAYSIA

DETERMINING THE MULTI-CURRENT SOURCES OF  
MAGNETOENCEPHALOGRAPHY BY USING FUZZY TOPOGRAPHIC  
TOPOLOGICAL MAPPING

WAN ENY ZARINA BINTI WAN ABDUL RAHMAN

A thesis submitted in fulfilment of the  
requirements for the award of the degree of  
Doctor of Philosophy

Faculty of Science  
Universiti Teknologi Malaysia

FEBRUARY 2006

To those who have affected my life in the most wondrous way;

My parents,  
Haji Wan Abdul Rahman Haji Hussein  
Hajjah Ashah Ibrahim

My husband,  
Mohd Fisol Hj Saud

My children,  
Nur Diyana, Nur Dalila, Nur Farah Ellyana,  
Nur Nadia Maisarah, Muhammad Arief,  
Nur Fatin Syahirah

My friends

and

My students

## ACKNOWLEDGEMENTS

Praise be to Allah, the Almighty for giving me the strength and courage to embark on this journey. Also for showering me a good experience and a wide exposure throughout this study period. And above all, for all that has been bestowed on me.

I would like to express my sincerest appreciation and gratitude to my supervisor, Assoc. Prof. Dr Tahir Ahmad and co-supervisor, Assoc. Prof. Dr Rashdi Shah Ahmad for the continuous guidance, support, encouragement and supervision throughout the research. Their advice and suggestions have been crucial for the success of this work.

My appreciation is also extended to Prof. Jim Bezdek (University of Western Florida) and Dr Lonnie C. Ludeman (New Mexico State University) for their valuable advice and suggestions. I am also very grateful to the laboratory assistants in UTM for accommodating me in the physics laboratory.

Special thanks goes to my colleagues, Assoc. Prof. Dr Arsmah Ibrahim and Assoc. Prof. Dr Daud Mohamad for giving me valuable advice, constructive criticisms and suggestions. Not forgetting too, my friends Salemah, Atie, Fauziah, Dr Ismail, Fadhil, Rosmawati, Aina and Ireen for all the support and friendship. To my family, I thank them for their love and understanding and most of all for putting up with my limited time I spent with them.

Finally, I am most grateful to University Technology MARA for granting the scholarship during my study.

## ABSTRACT

The human brain is an extremely complex system performing demanding information processing tasks rapidly. It consists of billions of neurons, each connected to others through thousands of synapses or interconnections. This huge network has many electric and chemical processes that can be measured in various ways. Magnetoencephalography (MEG) is a technique of measuring and recording the minute and very weak magnetic fields generated by the currents in the neurons. There are two types of problems in MEG, the forward problem and the backward or the inverse problem. The forward problem deals with finding the magnetic fields when the current source distribution is given or known. On the other hand, the inverse problem is to find the neural current source distribution given a series of magnetic fields measurements. This study has proposed the model FTTM2 (Fuzzy Topographic Topological Mapping Version 2) which is an extension to the novel mathematical modeling FTTM1 (Fuzzy Topographic Topological Mapping Version 1). The model FTTM2 comprises four components namely the Image Contour Plane (IC), Base Image Plane (BI), Fuzzy Image Field (FI) and Topographic Image Field (TI). In the process of applying FTTM2, emphasis is made on its first component, the IC where two different algorithms are being applied to the data. The first is the fuzzy *c*-means (FCM) algorithm which is used to determine the region where the current sources lie and also to approximate the number of current sources. The second is the seed-based region growing (SBRG) algorithm which is used to confirm the number of current sources available in the system by automation. Two theorems and three corollaries are derived and proven as theoretical basis of the proposed system. Finally, FTTM2 is tested on the generated and experimental data and subsequently verified using forward and backward calculations.

## ABSTRAK

Otak manusia adalah suatu struktur yang kompleks yang melaksanakan pemrosesan maklumat dengan tangkas. Otak terdiri daripada ribuan juta neuron yang berkait antara satu sama lain melalui ribuan jaringan. Jaringan ini pula mengandungi banyak proses elektrik dan kimia yang boleh diukur dengan pelbagai cara. Magnetoencephalography (MEG) adalah suatu teknik mengukur dan merekod medan magnet yang amat kecil dan lemah yang dihasilkan oleh arus yang mana arus itu pula terhasil oleh tindakan neuron. Terdapat dua permasalahan di dalam MEG iaitu masalah ke hadapan dan masalah ke belakang. Masalah ke hadapan melibatkan pengiraan medan magnet apabila kedudukan arus diketahui. Sebaliknya, pengiraan ke belakang melibatkan pengiraan kedudukan arus apabila hanya nilai-nilai medan magnet diketahui. Penyelidikan ini telah mengesyorkan model FTTM2 (*“Fuzzy Topographic Topological Mapping Version 2”*) yang mana ia adalah model yang telah diunjurkan dari FTTM1 (*“Fuzzy Topographic Topological Mapping Version 1”*). Model FTTM2 ini terdiri dari empat komponen iaitu *Image Contour Plane (IC)*, *Base Image Plane (BI)*, *Fuzzy Image Field (FI)* dan *Topographic Image Field (TI)*. Dalam proses mengaplikasikan FTTM2, tumpuan diberikan pada komponen pertama (*IC*) yang mana dua algoritma berbeza digunakan. Algoritma pertama ialah penggunaan *fuzzy c-means* (FCM) yang dapat menentukan lokasi bagi kedudukan arus dan dapat menganggarkan bilangan arus. Algoritma yang kedua melibatkan penggunaan *seed-based region growing* (SBRG) yang berupaya menentupastikan bilangan arus secara automasi. Untuk menguji kebolehgunaan kedua-dua algoritma ini, dua teorem beserta tiga korolari diterbitkan dan dibuktikan. Akhir sekali, FTTM2 diujikan ke atas data yang diperolehi dari simulasi dan juga dari ujikaji dan seterusnya dibuktikan dengan pengiraan ke depan dan ke belakang.

## TABLE OF CONTENTS

CHAPTER	TITLE	PAGE
	THESIS STATUS DECLARATION	
	SUPERVISOR'S DECLARATION	
	TITLE PAGE	i
	DECLARATION	ii
	DEDICATION	iii
	ACKNOWLEDGEMENTS	iv
	ABSTRACT	v
	ABSTRAK	vi
	TABLE OF CONTENTS	vii
	LIST OF TABLES	xiii
	LIST OF FIGURES	xvi
	LIST OF SYMBOLS AND ABBREVIATIONS	xxiv
	LIST OF APPENDICES	xxix
 <b>1</b>	 <b>INTRODUCTION</b>	 <b>1</b>
	1.1 Introduction	1
	1.2 Background of the Research	6
	1.3 Objective and Scope of Study	10
	1.4 The Significance of this Research	11
	1.5 Research Framework	12
	1.6 Outline of Presentation	14

<b>2</b>	<b>MAGNETOENCEPHALOGRAPHY</b>	<b>17</b>
2.1	Introduction	17
2.2	Electric Neural Activity	18
2.3	Current Dipole Model	22
2.4	Pattern Generated by a Current Dipole	24
2.5	Localization of Single Current Dipole	25
2.6	Detection of Magnetic Fields	26
2.6.1	The Forward Problem	27
2.6.2	The Backward Problem	28
2.7	Two Classes of Signals	28
2.8	Fuzzy Topographic Topological Mapping Version 1 (FTTM1)	32
<b>3</b>	<b>MATHEMATICAL BACKGROUND</b>	<b>38</b>
3.1	Introduction	38
3.2	Magnetism	38
3.2.1	Magnetic Field Intensity	43
3.2.2	Material Permeability	43
3.2.2.1	Biot-Savart's Law	43
3.2.3	The Magnetic Fields Effects	47
3.3	Crisp Set	49
3.3.1	Crisp Set Operations	50
3.4	Fuzzy Set	54
3.4.1	Fuzzy Set Operations	57
3.5	Image Processing	60
3.5.1	Neighbors of a Pixel	63
3.5.2	Connectivity	65



3.5.3	Regions	66
3.5.4	Segmentation	66
3.5.5	Image Enhancement	67
3.6	Feature Extraction	67
3.7	Region Growing	67
3.8	Clustering	68
3.8.1	Fuzzy c-Means (FCM) Clustering	69
3.8.2	FCM Algorithm	70
3.8.3	Cluster Validity	74
<b>4</b>	<b>MATHEMATICAL FORMULATION</b>	<b>78</b>
4.1	Introduction	78
4.2	The Axis Convention	78
4.3	Coordinates Transformation	79
4.4	Two-Dimensional Representation of the Magnetic Fields	82
4.5	The Measurement of Magnetic Field Lines	88
4.6	Mathematical Formulation	91
4.7	Acquisition of the Magnetic Fields Data	95
4.7.1	Generating the Magnetic Field Lines	97
4.7.1.1	Single Current Source (Segment)	97
4.7.1.2	Double Current Sources (Segments)	98

4.8	The Contour Plots of the Magnetic Fields for Single Current Source	98
4.8.1	Approximate Current Location	101
4.8.2	The Direction of Current Flow	102
4.8.3	The Orientation of Current	102
4.9	The Contour Plots of Multiple Current Sources	103
4.10	Constraints in Generating the Magnetic Fields Data	107
4.11	The Characteristics of Magnetic Fields Data on the Measurement Plane	107
4.11.1	The Magnetic Fields for a Single Current Source	107
4.11.2	Magnetic Fields for Double Current Sources	108
<b>5</b>	<b>THE FUZZY TOPOGRAPHIC TOPOLOGICAL MAPPING VERSION 2 (FTTM2) ALGORITHM</b>	<b>117</b>
5.1	Introduction	117
5.2	Fuzzy Topographic Topological Mapping Version 2 (FTTM2)	117
5.3	Image Contour Plane	123
5.3.1	Data Pre-Processing	124
5.3.1.1	Data Conversion to their Absolute Values	124
5.3.1.2	The Transformation of Magnetic Fields Data to Image Data	125

5.3.2	The Application of Fuzzy $c$ -Means (FCM) Algorithm	126
5.3.3	The Application of Seed-Based Region Growing (SBRG) Algorithm	128
5.4	Base Image Plane	129
5.5	Fuzzy Image Field	130
5.6	Topographic Image Field	131
5.6.1	Defuzzification of $\mu_{I_z}$	131
5.6.2	View of $Z$ in Three-Dimensions	133
5.6.3	The Inclination of Current Segments	133
5.6.4	Magnitude of Current Flow	133
5.6.4.1	Magnitude of Current for a Single and Bounded Current Segment	133
5.6.4.2	Magnitude of Current for Multiple Bounded Current Segments	134
5.7	Algorithm in FTTM2	134
<b>6</b>	<b>FCM AND SBRG ON FTTM2: THEORETICAL EMBEDDING</b>	<b>139</b>
6.1	Introduction	139
6.2	Topology Preliminaries	141
6.3	FCM and SBRG on Topological Spaces	142
6.4	FCM and SBRG on FTTM2	144
<b>7</b>	<b>IMPLEMENTATION</b>	<b>147</b>
7.1	Introduction	147
7.2	The Implementation Process	154

7.2.1	The Generated Data	154
7.2.1.1	Measurement on the Top of the Head, $\mathbf{B}_z$	154
7.2.1.2	Measurement on the Left Side of the Head, $\mathbf{B}_{y(\text{left})}$	194
7.2.1.3	Measurement on the Right Side of the Head, $\mathbf{B}_{y(\text{right})}$	205
7.2.2	The Experimental Data	212
7.2.2.1	Experimental Set-up	214
7.2.2.2	Measuring The Experimental Data	216
7.2.2.3	Limitations of the Experimental Works	230
7.3	Results for other Datasets	232
7.3.1	Results from the Generated Data	232
7.3.2	Results from the Experimental Data	234
<b>8</b>	<b>CONCLUSION</b>	<b>236</b>
8.1	Summary of Research	236
8.2	Significant Contributions	238
8.3	Suggestions for Future Research	238
	<b>REFERENCES</b>	<b>241</b>
	Appendices A to E	252-271

## LIST OF TABLES

TABLE NO.	TITLE	PAGE
7.1	The implementation table	149
7.2	The magnetic fields data, $B_z \times 10^{-5}$ (Tesla) measured on the top of the head	154
7.3	The absolute values of the magnetic fields data from Table 7.2	157
7.4	The image data	158
7.5	The matrix of features of size 3 by 256 for Feature Type 1	161
7.6	The matrix of features of size 3 by 196 for Feature Type 2	164
7.7	The matrix of features of size 7 by 196 for Feature Type 3	168
7.8	The cluster validity measures	181
7.9	The sample of the fuzzified data, $\mu_I$	183
7.10	The defuzzified data, $Z$	184
7.11	The table of $\max(Z)$ from columns 1 to 11 of Table 7.10	188
7.12	The angles of inclination for the current segment for measurement of the magnetic fields made on the $xy$ -plane (the top of the head)	191
7.13	The calculated current magnitude	192

7.14	The magnetic fields data, $\mathbf{B}_{y(\text{left})}$ measured on the left side of the head	194
7.15	The image data for measurements made on the left side of the head	197
7.16	The defuzzified data, $Z$	202
7.17(a)	The angles of inclination for the current segment 1 (S1)	204
7.17(b)	The angles of inclination for the current segment 2 (S2)	205
7.18	The magnetic fields data, $\mathbf{B}_{y(\text{right})}$ measured on the right side of the head	206
7.19	The image data	208
7.20(a)	Sample data of magnetic fields $B_c$ measured in the presence of current flowing	217
7.20(b)	Sample data of magnetic fields $B_0$ measured in the absence of current flowing	218
7.20(c)	Sample of the net magnetic fields, $B_n = B_c - B_0$	219
7.20(d)	The magnetic field data where each data is multiplied by $10^{-7}$	220
7.21	The image data	223
7.22	The defuzzified data, $Z$	225
7.23	The table of $\max(Z)$ from columns 1 to 9 of Table 7.22	226
7.24	The angles of inclination for the current segment where the measurement of the magnetic fields are made on the $xz$ -plane (the top of the head)	229

7.25	The magnitude of current	231
7.26(a)	The results for current segment 1 (S1)	233
7.26(b)	The results for current segment 2 (S2)	233
7.27	The results for the angles of inclination	234
7.28	The angles of inclination	235

## LIST OF FIGURES

<b>FIGURE NO.</b>	<b>TITLE</b>	<b>PAGE</b>
1.1	The important parts of the human brain (left side)	2
1.2	(a) Schematic illustration of a pyramidal neuron and three magnified synapses, (b) pyramidal neuron	3
1.3	Detection of cerebral magnetic fields using a SQUID magnetometer	6
1.4	The forward neuromagnetic modeling	8
1.5	The inverse neuromagnetic modeling	8
1.6	Inverse neuromagnetic modeling: FTTM1	9
1.7	Fuzzy Topographic Topological Mapping Version 1 (FTTM1)	10
1.8	Research framework	13
1.9	Thesis outline	16
2.1	Schematic representations of the intracellular and extracellular currents associated with the depolarization front of the action potential	19
2.2	A schematic picture of the electrical currents during (a) a propagating action potential, (b) a terminating action potential, and (c) a postsynaptic potential	20
2.3	The orientation of the pyramidal cells in the cortex	21
2.4	Magnetic fields of a current dipole in a homogeneous conducting medium	23



2.5	The contour plot of a current dipole	24
2.6	An example of the topographic field map calculated from the measured MEG signals	25
2.7	The magnetic field readings of environmental noise and human organs	27
2.8	Fuzzy Topographic Topological Mapping Version 1 (FTTM1)	34
3.1	The magnetic field lines around a magnet	39
3.2	The magnetic field lines surrounding a conductor	40
3.3	The direction of the magnetic fields lines using the right-hand rule	41
3.4	The direction of the magnetic fields for current flowing “into” the page	42
3.5	The direction of the magnetic fields for current that emerges “out of” the page	42
3.6	The current segment AC	44
3.7	Two currents flowing in the opposite directions	48
3.8	Two currents flowing in the same direction	49
3.9	Operations on crisp sets	52
3.10	Membership function of fuzzy set	56
3.11	Fuzzy number $F_2 = \{x \in \mathbb{R} : x \text{ is about } 4\}$	57
3.12	Operations on fuzzy sets	59
3.13	Fundamental steps in digital image processing	62
3.14	A $3 \times 3$ neighborhood about a point $(x, y)$ in an image	64

3.15	The four neighborhood of $(x, y)$ (4-neighbors)	64
3.16	Types of connectivity (a) 4-connectivity NSEW, (b) 6-connectivity NW/SE, (c) 6-connectivity NE/SW, (d) 8-connectivity	65
4.1	The axis convention	79
4.2	The cylindrical and the Cartesian coordinates	81
4.3	The transverse section of the current segment	83
4.4	The plot of $\mathbf{B}_z$ against $y$	84
4.5	The relationship between the components in the Cartesian coordinate system and cylindrical coordinate system	85
4.6	The relationship between $r$ and its $y$ and $z$ -components	86
4.7	Schematic locations of the measurement planes	90
4.8	The locations of two current segments underneath the horizontal measurement plane	92
4.9	The node at $(0, 0)$	96
4.10(a)	The contour plots of a single bounded current segment with coordinates: $S1=[0.03, 0.07, -0.01; 0.13, 0.07, -0.01]$	99
4.10(b)	The contour plots of a single bounded current segment with coordinates: $S1=[0.13, 0.07, -0.01; 0.03, 0.07, -0.01]$	99
4.10(c)	The contour plots of a single bounded current segment with coordinates: $S1=[0.03, 0.07, -0.05; 0.13, 0.07, -0.01]$	100
4.10(d)	The contour plots of a single bounded current segment with coordinates: $S1=[0.13, 0.07, -0.05; 0.03, 0.07, -0.01]$	100
4.10(e)	The contour plots of a single bounded current segment with coordinates: $S1=[0.10, 0.10, -0.01; 0.03, 0.03, -0.05]$	101

4.10(f)	The contour plots of a single bounded current segment with coordinates: $S1=[0.05, 0.05, -0.01; 0.13, 0.12, -0.05]$	101
4.11	The contour plots for two current segments at different locations as the distance between them decreases	104
4.12(a)	The contour plots for two bounded current segments, S1 and S2 with coordinates; $S1=[0.03, 0.03, -0.05; 0.13, 0.03, -0.01]$ and $S2=[0.03, 0.13, -0.05; 0.13, 0.13 -0.01]$	105
4.12(b)	The contour plots for two bounded current segments, S1 and S2 with coordinates; $S1=[0.02, 0.08, -0.01; 0.12, 0.02, -0.01]$ and $S2=[0.02, 0.08, -0.01; 0.12, 0.13 -0.01]$	106
4.12(c)	The contour plots for two bounded current segments, S1 and S2 with coordinates; $S1=[0.02, 0.08, -0.05; 0.12, 0.02, -0.01]$ and $S2=[0.02, 0.08, -0.05; 0.12, 0.13 -0.01]$	106
4.13	Magnetic fields measurements at locations C, D and E	108
4.14	Magnetic field measured at point M due to two current sources	109
4.15	The measurement point M located at equal distance between the current sources	112
4.16	Magnetic field measured at point M due to two current sources at different distances	113
4.17	Magnetic field measured at point M due to two current sources at different distances	114
4.18	Magnetic field measured at point M due to two current sources at different distances	115
4.19	Magnetic field measured at point M due to two current sources at different distances	116
5.1	The improved version of FTTM2	118
5.2	Fuzzy Topographic Topological Mapping Version 2 (FTTM2)	118
5.3	The transformation of FTTM1 to FTTM2	122

5.4	The linear stretching of magnetic fields data to image data	124
5.5	The possible ways for a seed pixel to grow using four-connectivity	128
5.6	The fuzzification graph	129
5.7	The defuzzification graph	131
6.1	The induced partition of A on B	143
6.2	The preservation of partitions from the first component to the fourth component	145
7.1	Flowchart of the implementation process	148
7.2	The $xy$ -plane where the measurement of $\mathbf{B}_z$ is made	151
7.3	The $xz$ -plane where the measurement of $\mathbf{B}_{y(\text{left})}$ is made	151
7.4	The $xz$ -plane where the measurement of $\mathbf{B}_{y(\text{right})}$ is made	152
7.5	The contour plot for the data $\mathbf{B}_z$ measured on the top of the head	155
7.6	The plot of $\mathbf{B}_z$ against $y$	156
7.7	The plot of the image data against $y$	159
7.8(a)	The clustered data C1	174
7.8(b)	The clustered data C2	174
7.9(a)	The clustered data C1	175
7.9(b)	The clustered data C2	175
7.10(a)	The clustered data C1	176

7.10(b)	The clustered data C2	176
7.11(a)	The clustered data C1	177
7.11(b)	The clustered data C2	178
7.11(c)	The clustered data C3	178
7.12(a)	The clustered data C1	179
7.12(b)	The clustered data C2	179
7.12(c)	The clustered data C3	180
7.12(d)	The clustered data C4	180
7.13	The output of the SBRG algorithm	182
7.14(a)	The 3-dimensional surface plot of the defuzzified data	185
7.14(b)	The 3-dimensional surface plot (rotated) of the defuzzified data depicting the valley between the two peaks	186
7.15	The plot of $\max(Z)$ values against $x$	189
7.16	The schematic diagram of the current segment below the measurement plane	189
7.17	The contour plot of the magnetic fields obtained from measurement at the left side of the head	195
7.18	The plot of data $\mathbf{B}_{y(\text{left})}$ against $z$	196
7.19	The plot of the image data against $y$	197
7.20(a)	The clustered data C1	198
7.20(b)	The clustered data C2	199
7.21	The output of the SBRG algorithm	200

7.22(a)	The surface plot	203
7.22(b)	The surface plot (rotated)	204
7.23	The contour plot as viewed from the right side of the head	207
7.24	The plot of data $\mathbf{B}_{y(\text{right})}$ against $y$	207
7.25	The plot of image data against $y$	209
7.26(a)	The clustered data C1	210
7.26(b)	The clustered data C2	210
7.27	The output of SBRG algorithm	211
7.28	The intersection of the three planes	212
7.29	The 520A fluxgate magnetometer	213
7.30	The fluxgate magnetometer probe (model APS 550 3 Axis)	213
7.31	Schematic diagram of the experimental set-up	215
7.32	Equipment set-up in the laboratory for measuring the magnetic fields	216
7.33	The contour plot of the magnetic fields obtained through experiments	221
7.34	The plot of $B_n$ against $y$	222
7.35	The plot of image data against $y$	223
7.36	The output of the SBRG algorithm	224
7.37	The surface plot of the defuzzified data	226
7.38	The plot of $\max(Z)$ against $x$	227

7.39	The schematic diagram of the current segment below the measurement plane	228
7.40	The contour plots of magnetic fields on (a) the top of the head, (b) left side of the head and (c) right side of the head	232
7.41	The contour plots for the experimental data	234
7.42	The contour plots for the experimental data	235

## LIST OF SYMBOLS AND ABBREVIATIONS

### General symbols

$A, B, C, \dots$	- Arbitrary set (crisp or fuzzy)
$A = B$	- Set equality
$A \neq B$	- Set inequality
$A \subset B$	- Proper set inclusion
$A \subseteq B$	- Set inclusion
$A \cap B$	- Set intersection
$A \cup B$	- Set union
$A \setminus B$	- Set difference
$[a, b]$	- Closed interval of real numbers between $a$ and $b$
$(a, b]$	- Interval of real numbers open in $a$ and closed in $b$
$[a, b)$	- Interval of real numbers closed in $a$ and open in $b$
$(a, b)$	- Open interval of real numbers between $a$ and $b$
$G_{min}$	- The smallest possible gray level value
$G_{max}$	- The largest possible gray level value
$\{x_1, x_2, x_3, \dots\}$	- Set of elements $x_1, x_2, x_3, \dots$
$\{x : p(x)\}$	- Set determined by property $p$
$(x_1, x_2, x_3, \dots)$	- $n$ -tuple
$i, j, k, \dots$	- Arbitrary identifiers (indices)
$N_4(p)$	- The 4-neighbours of $p$
$[x_{ij}]$	- Matrix
$\in$	- Element of
$\notin$	- Not an element of
$\exists$	- There exist (at least one)



$\forall$	- For all
$\Re$	- Set of real numbers
$\Re^n$	- Set of n-tuple of real numbers
$U$ or $X$	- Universal set
$\emptyset$	- Empty set
$\mu_A(x)$	- Membership grade of $x$ in fuzzy set A
$\ \dots\ $	- Euclidean norm
$(D\dots)$	- Definition
$\wedge$	- Intersection of two fuzzy sets
$\vee$	- Union of two fuzzy sets
$\min[x_1, x_2, x_3, \dots, x_n]$	- Minimum of $x_1, x_2, x_3, \dots, x_n$
$\max[x_1, x_2, x_3, \dots, x_n]$	- Maximum of $x_1, x_2, x_3, \dots, x_n$
$m$	- The weighting exponent
$U$	- Fuzzy partition matrix
$V = \{v_1, v_2, v_3, \dots, v_c\}$	- Set of cluster centres

## Magnetism

$\mathbf{B}_z$	- The magnetic fields data measured on the top of the head (at $z = 0$ )
$\mathbf{B}_{y(\text{left})}$	- The magnetic fields data measured on the left side of the head (at $y = 0$ )
$\mathbf{B}_{y(\text{right})}$	- The magnetic fields data measured on the right side of the head (at $y = 0.15$ )
$\mu_0$	- The permeability in free space
$\mu$	- Material permeability
$I$	- The magnitude of current flow in a conductor
$\theta_1$	- The angle between a line parallel to the segment in the direction of the current flow and the line joining the starting point of the segment A to the measurement point
$\theta_2$	- The angle between a line parallel to the segment in the direction of the current flow and the line joining the end point of the current segment to the measurement point

$r$	- The perpendicular distance between the current source and the measurement point on a plane
$\hat{\mathbf{r}}$	The unit perpendicular distance
$BZ$	- The absolute value of $B_z$
$\max(BZ)$	- The maximum value of $BZ$
$\min(BZ)$	- The minimum value of $BZ$
$\max(\max(BZ))$	- The maximum among all the maximum values of $BZ$
$\min(\min(BZ))$	- The minimum among all the minimum values of $BZ$
$I_z$	- The image data in the range of [0, 255]
$\max(I_z)$	- The maximum value of the fuzzified data
$\min(I_z)$	- The minimum value of the fuzzified data
$\mu_{I_z}$	- The fuzzified image data in the range [0, 1]
$\mu_{B_z}$	- The fuzzified magnetic fields values in the range [0, 1]
$x, y, z$	- Cartesian coordinates
$B_x$	- The x-component of the magnetic fields
$B_y$	- The y-component of the magnetic fields
$B_0$	- The magnetic fields data when current is not flowing
$B_c$	- The magnetic fields data when current is flowing
$B_n$	- The net magnetic fields data obtained from the difference between $B_c$ and $B_0$
$h$	- The distance between the current source and the measurement plane
$d$	- The distance between the two extrema of the magnetic field contours
$Z$	- The defuzzified values

<b>B</b>	- Magnetic fields vector
<b>H</b>	- Magnetic field intensity
$\hat{\mathbf{a}}_\phi$	- The unit vector along the concentric circular path of the magnetic field lines
$\hat{\mathbf{a}}_r$	- The unit vector along the perpendicular line from the line current to the field point
$\hat{\mathbf{a}}_I$	- The unit vector along the line current

### Abbreviations

MEG	- Magnetoencephalography
SQUID	- Superconducting Quantum Interference Device
FTTM1	- Fuzzy Topographic Topological Mapping Version 1
FTTM2	- Fuzzy Topographic Topological Mapping Version 2
FCM	- Fuzzy c-Means
SBRG	- Seed-Based Region Growing
MC	- Magnetic contour plane
BM	- Base magnetic plane
FM	- Fuzzy magnetic field
TM	- Topographic magnetic field
IC	- Image contour plane
BI	- Base image plane
FI	- Fuzzy image field
TI	- Topographic image field
ROI	- Region of interest
S1	- Current segment 1
S2	- Current segment 2
MUSIC	- Multiple signal classification
FEM	- Finite element method
BEM	- Boundary element method
ICA	- Independent component analysis

ECD	-	Equivalent current dipole
SEFs	-	Somatically evoked magnetic fields
VEFs	-	Visually evoked magnetic fields
PC	-	Partition coefficient
PE	-	Partition entropy
Prop_E	-	Proportion exponent
CSV	-	Compactness and separation validity
PSPs	-	Postsynaptic potentials
MNE	-	Minimum norm estimates
LHe	-	Liquid helium
RHR	-	Right-Hand Rule
MLE	-	Maximum likelihood estimation

**LIST OF APPENDICES**

<b>APPENDIX</b>	<b>TITLE</b>	<b>PAGE</b>
A1	Flowchart 1	252
A2	Flowchart 2	253
A3	Flowchart 3	254
A4	Flowchart 4	255
A5	Flowchart 5	256
A6	Flowchart 6	257
A7	Flowchart 7	258
B	Flowchart 8	259
C	Flowchart 9	260
D1	Flowchart 10	261
D2	Flowchart 11	262
D3	Flowchart 12	263
D4	Flowchart 13	264
E	Trends of the results	265
F	Papers Published	272

## CHAPTER 1

### INTRODUCTION

#### 1.1 Introduction

The human brain is the most important organ in our body. It is also the most sophisticated creation known to exist. Therefore, understanding how the brain works is one of the greatest challenges ever faced by mankind. The brain fulfills several important functions such as processing of sensory information, the programming of motor and emotional responses, the storage of information and learning. These complex tasks are carried out by the interconnected sets of neurons. There are at least  $10^{10}$  neurons in the outermost layer of the brain, the cerebral cortex (Penfield and Rasmussen, 1950). This is the part which differs most from the brain of other animals (Devinsky, 2001). This cerebral cortex is a greatly convoluted sheet of cells, about 3 mm thick, consisting of small grooves (sulci), large grooves (fissures) and bulges between them (gyri). The neurons are the active cells units in a vast signal handling network, which include  $10^{14}$  interconnections or synapses. When information is being processed, small currents flow in the neural system and produced a weak magnetic field, which can be measured noninvasively by a device known as Superconducting Quantum Interference Device (SQUID) magnetometer, placed outside the skull, provided that thousands of nearby neurons act synchronously (Hamalainen *et al.*, 1993).

The brain consists of two hemispheres, separated by the longitudinal fissure. The left and right halves, in turn are divided into lobes by two deep grooves. The Rolandic fissure runs down the side of both hemispheres, while the Sylvian fissure is almost horizontal (see Figure 1.1). There are four lobes in both halves of the cortex: frontal, parietal, temporal and occipital. Each lobe contains many different areas that have different functions. Most regions of the cortex have been mapped functionally (Hamalainen *et al.*, 1993). Figure 1.1 below shows some of the important structural landmarks and special areas of the cerebral cortex.

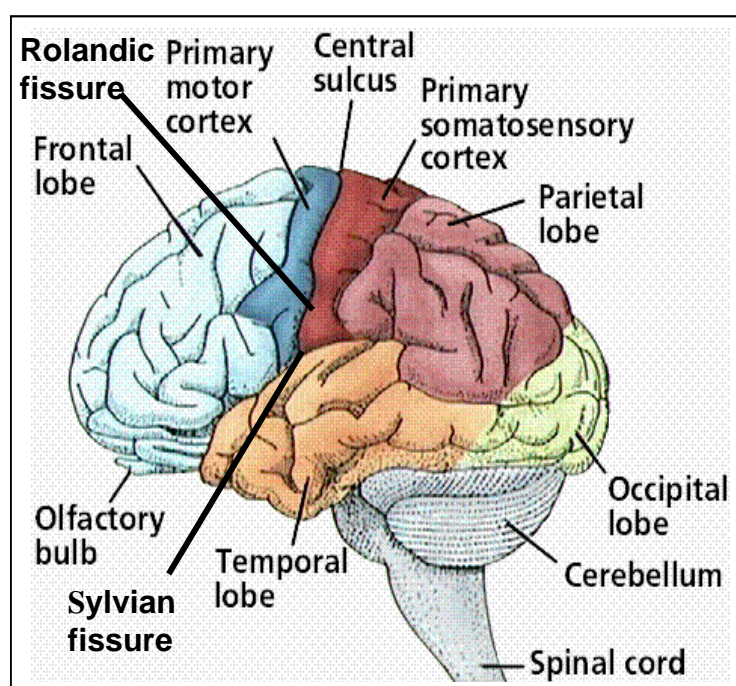


**Figure 1.1** The important parts of the human brain (left side)

The primary somatosensory cortex, which receives tactile stimuli from the skin, is located posterior to the Rolandic fissure. The area in the frontal lobe just anterior to the Rolandic fissure contains neurons concerned with the integration of muscular activity: each site of the primary motor cortex is involved in the movement of a specific part of the body (Hamalainen *et al.*, 1993).

The nervous system is the most complex and delicate of all the body systems. At the center of the nervous system is the brain. The brain sends and receives messages through a network of nerves. These nerve cells or the neurons are the basic functional unit of the nervous system. Figure 1.2 is an illustration of the structure of the neuron.

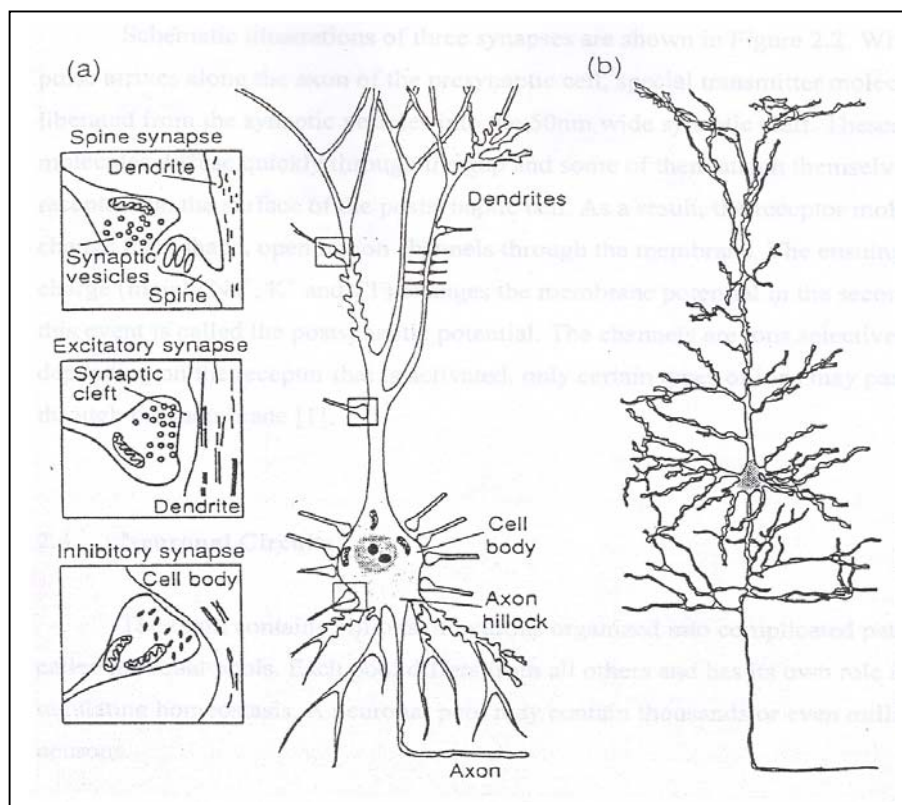


**Figure 1.2** (a) Schematic illustration of a pyramidal neuron and three magnified synapses, (b) pyramidal neuron (Hamalainen *et al.*, 1993).

The neuron is a nerve cell specialized for the reception, interpretation and the transmission of electrical messages. They function like computer chips, analyzing and processing information and then sending signals through the nerve fibers. Basically, a neuron consists of a cell body that receives electrical messages from other neurons through contacts called synapses located on the dendrites or on the cell body. The dendrites are the parts of the neuron specialized for receiving information from stimuli or from other cells. If the stimulus is strong enough, the neurons transmit an electrical signal outward along a fiber called an axon. The axon or nerve



fibre, which may be as long as 1 meter carries the electrical signal to the muscles, glands or other neurons.

The two principal groups of cortical neurons are the pyramidal and the stellate cells. The former are relatively large; their apical dendrites from above reach out parallel to each other, so that they tend to be perpendicular to the cortical surface. Since neurons guide the current flow, the resultant direction of the electric current flowing in the dendrites is also perpendicular to the cortical sheet of gray matter.

In the human brain, there are more than several hundred millions of neurons connecting with each other and working for auditory and visual information processing. In these neurons, ion currents flow while these neurons are involved in the information processing. The ion current goes out of the neurons and flows in the conductive brain. It is these ion currents that produce the magnetic fields which flows according to the Right-Hand Rule (RHR) (Sadiku, 1995). Amazingly, this magnetic field can emerge out of the head through the brain, the skull, the cerebrospinal fluid and the scalp without receiving any distortion. This outstanding characteristic of magnetic fields becomes important in the studies of Magnetoencephalography (MEG).

MEG is a revolutionary medical imaging technology that provides unprecedented insight into the workings of the human brain through the measurement of electromagnetic activity. It is a technique of recording and measuring the minute and very weak magnetic fields produced by electrical activities in the brain (Hamalainen *et al.*, 1993). By measuring the magnetic fields created by the electric current flowing within the neurons, MEG identifies brain activities associated with various functions in real time with millimeter spatial accuracy. MEG is also completely non-hazardous since the human subject is not exposed to x-rays, radioactive tracers or to time-varying and strong static magnetic fields. Furthermore, MEG is noninvasive since it permits studies of the brain without opening the skull.

Different parts of the brain produce different patterns of magnetic waves (signals). Diseased brains can produce abnormal magnetic signals. The special feature of MEG is that it can be used to determine which brain regions are malfunctioning. It can also identify specific foundation regions of the brain such as auditory and visual cortex. Stimuli such as sounds or pictures will activate specific portions of the brain in characteristic sequences. MEG examines neuromagnetic (a near synonym of MEG, meaning the study of neuronal activity by means of magnetic fields) activity changes during this stimulation and pinpoints the location of functional regions. This helps determine if the sequence of activation has been perturbed by disease. MEG can be used to accurately localize sources within the brain. This information is useful in the field of medicine especially for pre-surgical functional mapping assessment of pathological functional deficits, neuropharmacological investigations, trauma assessment and a growing list of research investigations in neuroscience and psychiatry. Furthermore, by using MEG, one can measure the activity of the brain in real time. This means that the brain can be observed “in action” rather than just viewing a still image.

In MEG studies, the weak magnetic fields are measured with the sensitive device known as SQUID magnetometer. This device only works at a temperature of -270 degrees Celcius, which requires that it be kept in a large container of liquid helium. Figure 1.3 illustrates the arrangement of the magnetometer that is placed above a patient's head while the patient is in a lying position.

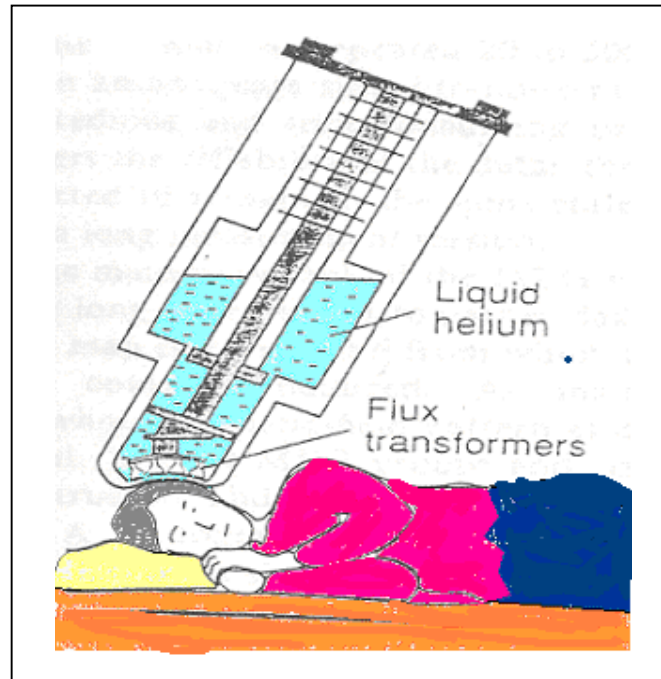


**Figure 1.3** Detection of cerebral magnetic fields using a SQUID magnetometer (Hamalainen *et al.*, 1993)

MEG measurements are normally carried out inside a special magnetically shielded metal room. This is due to the fact that the magnetic signals from the brain are extremely weak as compared to the ambient magnetic field variations. Thus, the rejection of the outside disturbances is of utmost importance. Significant magnetic noise is caused for example, by fluctuations in the earth's geomagnetic field, moving vehicles and elevators, radio, television and microwave transmitters and the omnipresent power-line fields.

## 1.2 Background of the Research

The neurons in the brain normally generate electrochemical impulses that act on other neurons, glands, and muscles to produce human thoughts, feelings and actions. When there is any disruption of the electrical processes, the neurons may function abnormally. Epilepsy or seizure disorder is a condition in which clusters of

nerve cells, or neurons in the brain sometimes signal abnormally. In epilepsy, the normal pattern of neuronal activity becomes disturbed (Penfield and Jasper, 1954), causing strange sensations, emotions and behaviors, or sometimes convulsions, muscle spasms and loss of consciousness. During an epileptic seizure, neurons may fire as many as 500 times a second, much faster than the normal rate of about 80 times a second. These seizures can last anywhere from a few seconds to a few minutes, and are usually spontaneous and uncontrolled. According to Hari (1996), the first clinical application of MEG is in the determination of epileptic foci. Physiologically, the epileptic foci refer to the location of the current sources, which generate the corresponding magnetic fields.

In spite of advances in antiepileptic medication, seizures in some patients cannot be controlled adequately. About 10 % - 20 % of all epileptic patients ultimately suffer from medically intractable epileptic seizures (Yung and Hsiang, 2002). Neurologists often suggest surgery to resect the problematic cells. However, the surgery can never be successful unless treated at the exact location of those problematic cells. Hence, it is crucial to determine the epileptogenic focus precisely before choosing the surgical procedure, that is, a presurgical localization plays an essential role in neurosurgical planning. This is to avoid injury to the primary sensory-motor cortices during the procedures (Lueders *et al.*, 1983; Gallen *et al.*, 1995), thus reducing the risk of the patient being left with a permanent functional deficit such as paralysis or loss of speech and sensation. As MEG is an established technique that can measure and record the very weak magnetic fields, it can therefore be adopted to determine or locate the epileptogenic focus in epileptic patients. The weak magnetic fields produced by the cerebral electrical activities in the brain that occurs during epileptic seizure measured by the MEG can serve as a presurgical measure. The main purpose of measuring these magnetic fields is to locate the electrical activity and to determine its distribution in the brain (Risto *et al.*, 1994).

In MEG, there exist two types of problems involving the forward and the backward (inverse) problems. The forward problem involves calculating the observable variables (magnetic fields) caused by the current sources. On the other hand, the inverse problem involves estimating the location, orientation and the

magnitude of the current sources from the results of the magnetic fields measurements. These two problems can be presented using the corresponding models: the forward model and the backward model. Figure 1.4 below illustrates the forward model.

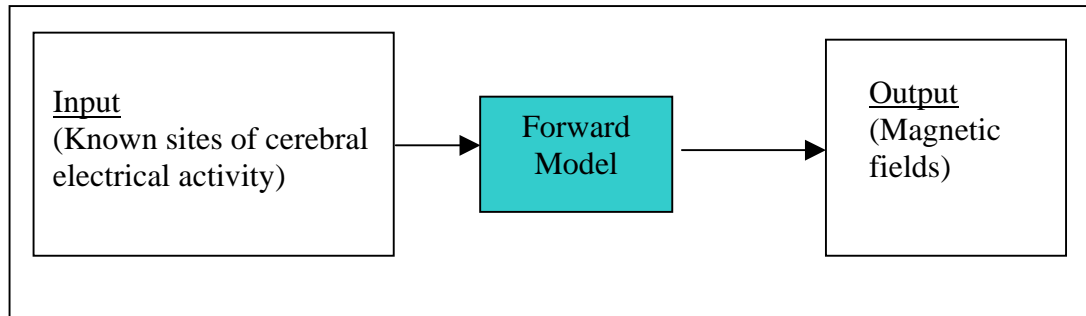


**Figure 1.4** The forward neuromagnetic modeling

The backward model is illustrated in Figure 1.5 below;

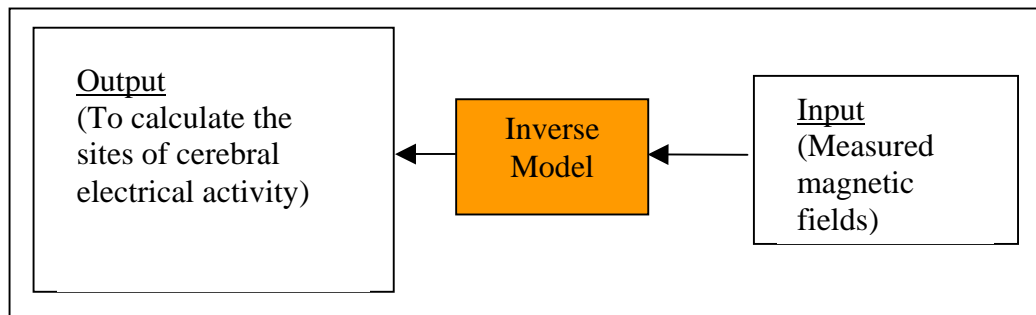


**Figure 1.5** The inverse neuromagnetic modeling

Until now, all methods used to solve the inverse problems depended on prior data. Clarke (1989), Hamalainen *et al.* (1993), Baillet and Garnero (1997), Philips *et al.* (1997) and Hasson and Swithenby (1999) applied the Bayesian approach, which allows the introduction of *a priori* information. Ricardo *et al.* (2000) applied the independent component approach (ICA) to the analysis of MEG recordings. Boris *et al.* (2004) and De Munck *et al.* (2004) used the maximum likelihood estimation (MLE) approach. These approaches are based on statistical methods that involve

loads of data. These kinds of models are also said to be the data-based models. Unfortunately, these models are limited by the computational burden where the computing time is unnecessarily long and hence makes the process of solving the problem tedious.

As opposed to the above model, Tahir *et al.* (2000) proposed a novel structured-based model known as Fuzzy Topographic Topological Mapping Version 1 (FTTM1). The FTTM1 model requires only instantaneous data. As a consequence of this, the computing time is consequently reduced, unlike the statistical-based models. Figure 1.6 illustrates the FTTM1 model, which is based on the backward model as illustrated in Figure 1.5.

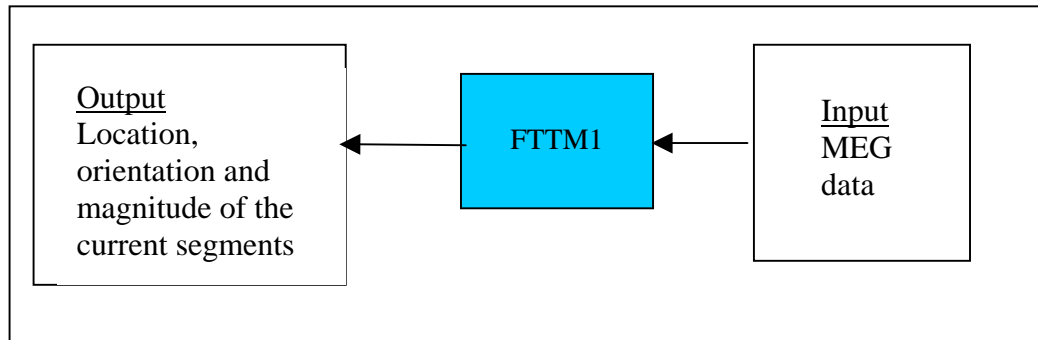


**Figure 1.6** Inverse neuromagnetic modeling: FTTM1

Basically, this newly developed model is a topological mapping which contains some fuzzy structures and it comprises four components linked by three different algorithms. The four components are magnetic contour plane (MC), base magnetic plane (BM), fuzzy magnetic field (FM) and topographic magnetic field (TM). Figure 1.7 illustrates the FTTM1 model;

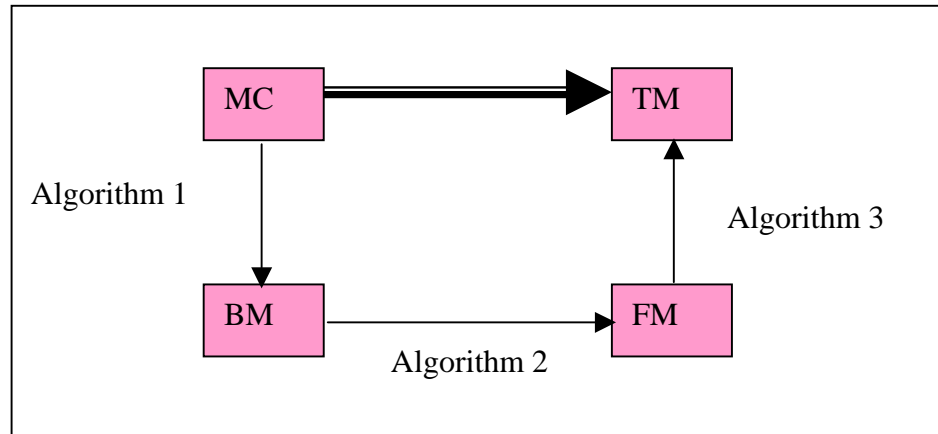


**Figure 1.7** Fuzzy Topographic Topological Mapping Version 1 (FTTM1)

Traditionally, the MEG data used for analyses are obtained using the SQUID measurements made above the head. However, to test the applicability of the newly developed model FTTM1, simulated data were used (Fauziah *et al.*, 2000). As the model is structured-based, it does not need *a priori* data and hence, it is anticipated that the computing time can be reduced. Initially, this model was applied to simulated data of single and unbounded current sources and has provided fairly good results (Fauziah, 2002).

In this research, an extended version of FTTM1 which will be known as FTTM2 is proposed. Unlike FTTM1, this new model uses image data, which are transformed from the magnetic fields data. The use of the image data is to incorporate the image processing techniques that will provide better visualization of the image. The model will then be used to solve the inverse problem of single bounded and multiple bounded current sources.

### 1.3 Objective and Scope of Study

The main objective of this study is to solve the backward (inverse) problem of MEG. This involves finding the location of the current sources from the measured magnetic fields. Physiologically, this implies finding the epileptic foci in epilepsy

disorder patients. Before the backward problem can be solved, the forward problem must first be taken care of. The forward problem deals with writing an algorithm to generate the magnetic fields data for multiple bounded current sources. This includes the generation of data measured at three different planes where this kind of measurement is especially useful for overlapping current sources. The magnetic fields data generated can then be used to find the parameters for multi-current sources. This includes the number of current sources present, the location of the current sources, its orientation and also its magnitude.

The newly proposed inverse model, FTTM2 is incorporated with a fuzzy clustering technique known as fuzzy *c*-means (FCM) and an image processing technique known as the seed-based region growing (SBRG). Because of the topological structure of FTTM2, it has the biggest advantage in that it can be applied anywhere on a patient's head (top or the sides). In other words, it is invariant with regards to the measured space in a given time. Consequently, new algorithms in solving the inverse problem of MEG are introduced. Since this study deals with testing the applicability of the newly developed inverse model, the scope of this study is limited to the use of simulated magnetic fields data obtained from single bounded and multiple bounded current sources. Experimental works are also undertaken to test the applicability as well as the performance of the developed model.

#### **1.4 The Significance of this Research**

This research adopts the techniques of image processing in solving the inverse problem of MEG. In doing so, a new model is formulated which can consequently be used to further enhance the applications of MEG. The new model, FTTM2, is a structured-based model. This implies that the model is constructed by studying the characteristics of the current sources and its corresponding magnetic fields. This model also uses instantaneous data which implies that the model does not require much time in providing the results.



Since the model is able to pinpoint the location of current sources, it will be useful in the presurgical localization of the current focus where only the problematic cells will be resected. Hence, this will give minimum or no side effects to the patients when undergoing surgery. This discovery serves as a significant contribution in the neurosurgical field specifically for epileptic disorder or any other problem areas analogous to it.

## **1.5 Research Framework**

This research comprises two main phases namely solving the forward problem and the backward problem. Solving the forward problem deals with generating the magnetic fields data. This will be accomplished by using MATLAB simulations and experimental work in the laboratory. The backward problem deals with using these data and applying the proposed model to determine the number of current sources, its location and also its magnitude. Figure 1.8 illustrates the general procedures. Data gathered by simulations and experiments in phase 1 are used in the second phase where FTTM2, incorporated with fuzzy *c*-means (FCM) and seed-based region growing (SBRG), is adopted to produce an output. This process produces the number of current sources, its location as well as its magnitude.

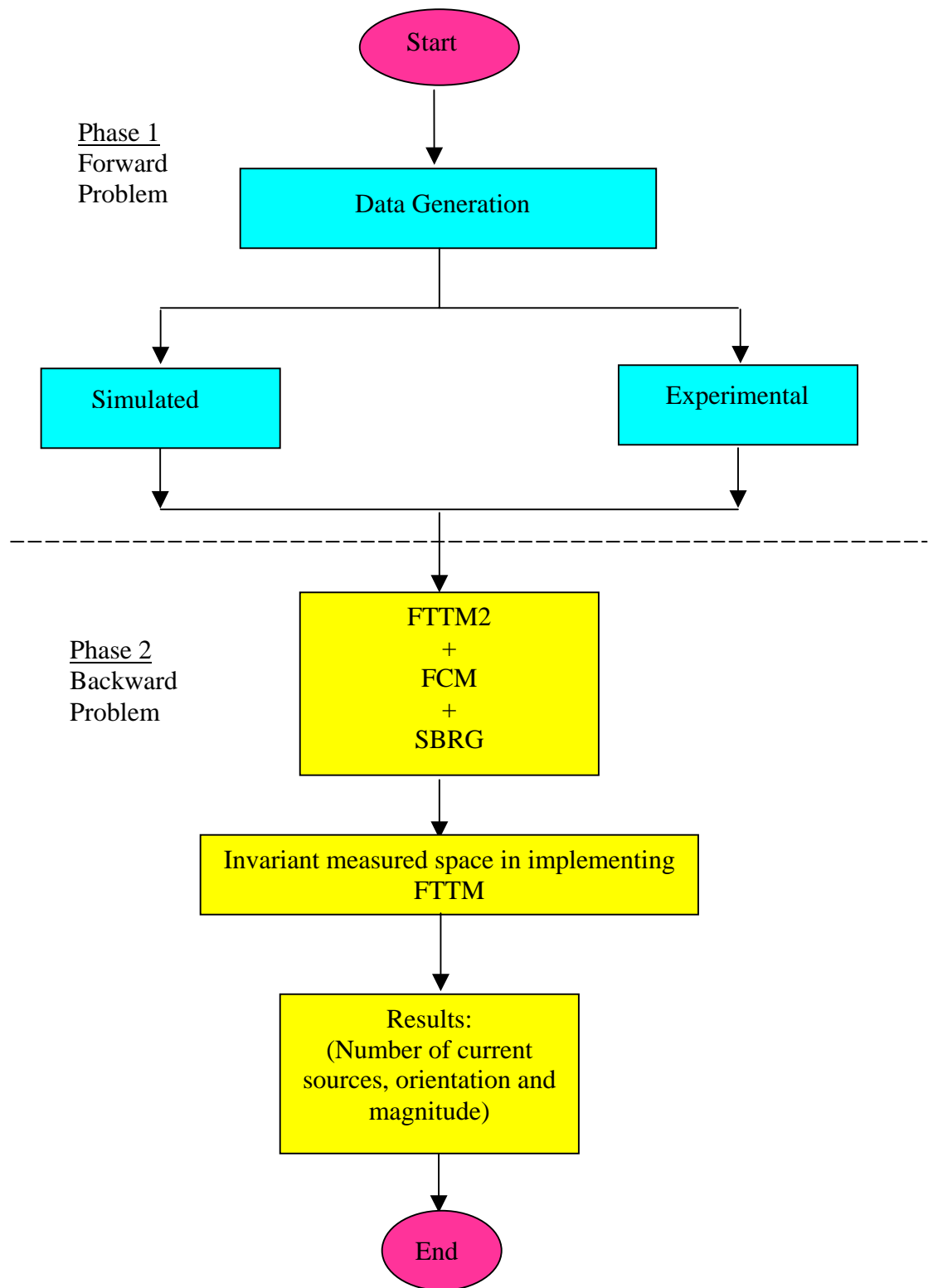


**Figure 1.8** Research framework

## 1.6 Outline of Presentation

This chapter gives an overview of the research undertaken. Chapter 2 begins with a review of previous studies on Magnetoencephalography, its measurement and the methods used to solve the forward and the inverse problems.

Chapter 3 explains the essential mathematical background that are used in this research. This includes substantial topics on magnetism, crisp set, fuzzy set, image processing, seed-based region growing and clustering.

The main contributions of this study are presented in the next four chapters. Chapter 4 describes the procedure to calculate the magnetic fields from known location of current sources. The detailed algorithms are given. In order to facilitate their uses, the algorithms are coded in MATLAB. The outputs of the algorithms are presented in the form of magnetic fields data and its corresponding contour plots. This is to examine the patterns generated with the associated known current location and orientation of the current sources. This information will be useful in solving the inverse problem later. In addition to this, the characteristics of the magnetic fields data are also examined by means of equations and geometries.

Chapter 5 describes the inverse model of FTTM2 in detail. This involves the use of a clustering algorithm known as fuzzy  $c$ -means (FCM) that is used to cluster the data into foreground and background regions. Another algorithm is the seed-based region growing (SBRG) which can be used to determine the number of current sources present in the system by automation. Once these two algorithms are applied, the data will be processed further by going through the other processes in FTTM2.

In Chapter 6, we propose the theoretical bases supporting Chapters 5 and 7 by proving two theorems and three corollaries. These theorems and corollaries showed that the partitioning applied to the first component is preserved during the transformation from the first component to the fourth component. Since this involves some concepts of topology, some preliminaries on topology are also

included. To verify these theorems and corollaries, they are implemented on the data as described in the next chapter.

The detailed implementation of the FTTM2 is illustrated in Chapter 7 where the topological structure of FTTM2 plays another main role in localizing the current sources. The implementation starts with the acquisition of magnetic fields data via two different methods. In the first method, the data is acquired through MATLAB simulations while in the second method, the data is acquired through laboratory experiments. These data acquisition is also called the forward calculations, which provides data to be used in solving the backward problem. In the backward problem, the data is then processed by applying FCM clustering algorithm and the SBRG algorithm and the developed FTTM2 algorithm. The results are also shown in this chapter.

Finally, Chapter 8 concludes the thesis with a summary of the study and recommendations for further research into this area of study. The thesis outline is summarized in Figure 1.9.

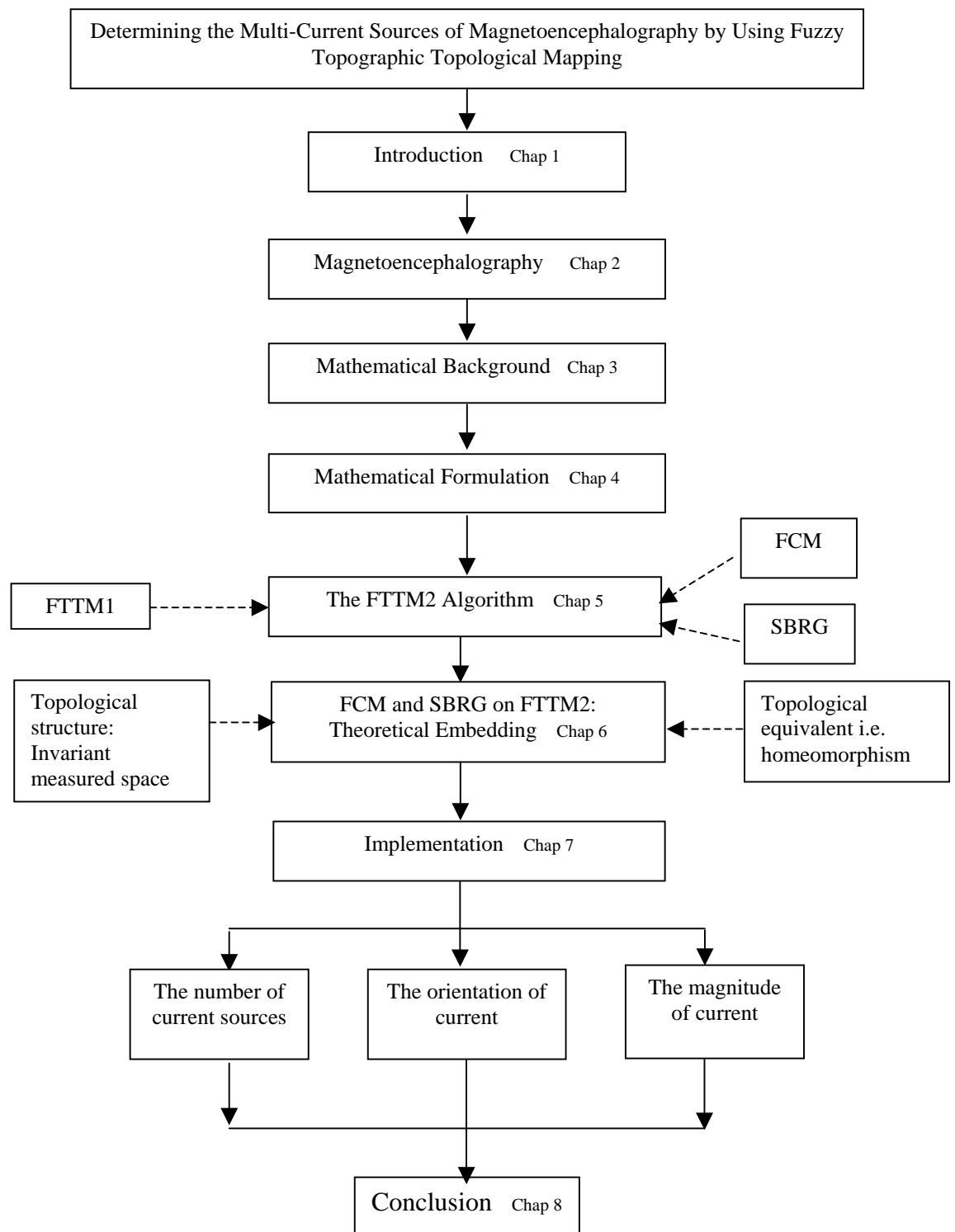


**Figure 1.9** Thesis outline

## REFERENCES

- Allenby, R.B.J.T. (1983). *Rings Fields and Groups: An Introduction to Abstract Algebra*. London : Edward Arnold.
- Amari, S. and Chichocki, A. (1998). Adaptive Blind Signal Processing-Neural Network Approaches. *Proc. IEEE*. 86: 2026-2048.
- Babuska, R., Setnes, M., Kaymak, U. and Vebruggen, H.B. (1997). Fuzzy Modeling: A Universal and Transparent Tool. *Proceedings of Toolmet*. Helsinki, Finland, 1-27.
- Baillet, S. and Garnero, L. (1997). A Bayesian Approach to Introducing Anatomic-Functional Priors in the EEG/MEG Inverse Problem, *IEEE Trans. Biom Eng.* 44: 374-385.
- Barth, D.S., Sutherling, W., Engel, Jr., J. and Beatty, J. (1982). Neuromagnetic Localization of Epileptiform Spike Activity in the Human Brain. *Science*. 218: 891-894.
- Bezdek, J. C. (1981). *Pattern Recognition with Fuzzy Objective Function Algorithms*. New York: Plenum Press.
- Bezdek, J. C., Ehrlich, R. and Full, W. (1984). FCM: The Fuzzy c-Means Clustering Algorithm. *Computers and Geosciences*. 10: 191-203.
- Bezdek, J.C., Hall, L.O. and Clark, L.P. (1993). Review of MR Image Segmentation Techniques using Pattern Recognition. *Medical Physics*. 20(4): 1033-1048.

- Bezdek, J.C., Hall, L.O., Clark, M. C., Goldgof, D.B. and Clark, L.P. (1997). Medical Image Analysis with Fuzzy Models. *Statistical Methods in Medical Research*. 3: 191-214.
- Birkhoff, G. and Bartee, T.C. (1970). Modern Applied Algebra. New York: McGraw Hill,
- Boris, V.B., Barry D. V. V. and Ronald, T.W. (2004). Maximum-Likelihood Estimation of Low-Rank Signals for Multiepoche MEG/EEG Analysis. *IEEE Trans. On Biomedical Eng.* 51(11): 1981-1993.
- Brenner, D., Lipton, J., Kaufman, L. and Williamson, S.J. (1978). Somatically Evoked Magnetic Fields of the Human Brain. *Science*. 199: 81-83.
- Brenner, D., Williamson, S.J. and Kaufman, L. (1975). Visually Evoked Magnetic Fields of the Human Brain. *Science*. 190: 480-482.
- Clarke, C.J.S. (1989). Probabilistic Methods in a Biomagnetic Inverse Problem. *Inverse Problem*. 5: 999-1012.
- Clarke C.J.S., and Janday, B.S. (1989). Probabilistic Methods in Biomagnetic Inverse Problem. *Inverse Problems*. 5: 483-500.
- Cohen, D. (1972). Magnetoencephalography: Detection of the Brain's Electrical Activity with a Superconducting Magnetometer. *Science*. 175: 664-666.
- Comon, P. (1994). Independent Component Analysis-A New Concept? *Signal Processing*. 36: 287-314.
- De Munck, J.C., Bijma, F., Gaura, P., Cezary, A. S., Brando, M.I. and Heethaar, R.M. (2004). A Maximum-Likelihood Estimator for Trial-to-Trial Variations in Noisy MEG/EEG Data Sets. *IEEE Transactions on Biomedical Engineering*. 51(12): 2123-2127.

- Devinsky, O. (2001). *Epilepsy: Patient and Family Guide*. 2<sup>nd</sup> Edition. Canada: F.A. Davis Co.
- Dugundji, J. (1975). *Topology*. New Delhi : Prentice Hall of India,.
- Eschrich, S., Ke, J., Hall, L.O., and Goldgof, D.B. (2001). Fast Fuzzy Clustering of Infrared Images, *Proceedings of the 20<sup>th</sup> NAFIPS International Conference*, Vancouver, Canada. 1145-1150.
- Fauziah Zakaria, Tahir Ahmad. dan Rashdi Shah Ahmad (2000). Pemodelan Isyarat Magnetoencephalography. *Prosiding Simposium Kebangsaan Sains Matematik Ke 8*, April 1-2, Terengganu, Malaysia. UPMT 202-210.
- Fauziah Zakaria (2002). *Algoritma Penyelesaian Songsang Bagi Arus Tunggal Tak Terbatas Magnetoencephalografi (MEG)*. Universiti Teknologi Malaysia: Tesis Sarjana.
- Gallen, C. C., Schwartz, B. J., Bucholz, R. D., Malik, G., Barkley, G. L., Smith, J., Tung, H., Copeland, B., Bruno, L., Assam, S., Hirschkoff, E., and Bloom, F. (1995). Presurgical Localization of Functional Cortex Using Magnetic Source Imaging. *Journal of Neurosurgery*. 82: 988-994.
- Giancoli, D. C. (2000). *Physics for Scientists and Engineers*, 3<sup>rd</sup> edition, Upper Saddle River, N.J.: Prentice Hall.
- Gonzalez, R.C. and Woods, R.E. (1992). *Digital Image Processing*. New York: Addison Wesley Publishing Company.



Hall, L.O., Amine, M.B. and Clarke, L.P. (1992). A Comparison of Neural Network and Fuzzy Clustering Techniques in Segmenting MR Images of the Brain. *IEEE Transactions on Neural Networks*, 3(5): 672-682.

Halliday, D. and Resnick, R. (1981). *Fundamentals of Physics*, 2<sup>nd</sup> edition. United States of America, John Wiley & Sons, 537-566.

Hamalainen M.S., Hari R., Illmoniemi R. J., Knuutila J. and Lounasmaa O.V. (1993). Magnetoencephalography-Theory, Instrumentation and Applications to Noninvasive Studies of the Working Human Brain, *Review of Modern Physics*. 65(2): 413-497.

Hamalainen, M.S. and Illmoniemi, R.J. (1994). Interpreting Magnetic Fields of the Brain: Minimum Norm Estimates. *Medical and Biological Engineering and Computing*. 35-42.

Hari, R. (1996). MEG in the Study of Human Cortical Functions, *Electroencephalography. And Clinical Neurophysiology*, 47: 47-54.

Hartigan, J.A. (1975). *Clustering Algorithms*, New York: John Wiley.

Hasson, R. and Swithenby, S.J. (1999). A Bayesian Test for the Appropriateness of a Model in the Biomagnetic Inverse Problem. *Inverse Problems*. 15: 1439-1454.

Heidi, W. (1999). *Neuromagnetic Studies on Somatosensory Functions in Healthy Subjects and Stroke Patients*. University of Helsinki, Academic Dissertation.

Hyvarinen, A. (1999). Survey on Independent Component Analysis. *Neural Computing Surveys*, 36: 94-128.

- Jain, A.K. (1989). *Fundamentals of Digital Image Processing*. Englewood Cliffs, N.J.: Prentice-Hall.
- Jain, R., Kasturi, R. and Schunk, B.G. (1995). *Machine Vision*. McGraw Hill.
- Janday, B. S. and Swithenby, S.J. (1987). Analysis of Magnetoencephalographic Data Using the Homogeneous Sphere Model: Empirical Tests. *Physics in Medicine and Biology*. 32(1): 105-113.
- Jutten, C. and Herault, J. (1991). Blind Separation of Sources. Part 1: An Adaptive Algorithm Based on Neuromimetic Architecture, *Signal Processing*, 24:1-10.
- Kallergi, M., Woods, K., Clarke, L.P., Wei, Q. and Clark, R. A. (1992). Image Segmentation in Digital Mammography: Comparison of Local Thresholding and Region Growing Algorithms. *Computerized Medical Imaging and Graphics*, 16(5): 323-331.
- Kandel, A. (1982). *Fuzzy Techniques in Pattern Recognition*. New York: John Wiley.
- Kandel, E.R., Schwartz, J.H. and Jessel, T.M. (1991). *Principles of Neural Science*. Norwalk, Connecticut: Appleton and Lange.
- Karp, P. (1981). Cardiomagnetism. In: Ernd, S.N., Hahlbohm, H.D., and Lobbig, H. Biomagnetism. Berlin: de Gruyter. 219-258.
- Klir, G.J. and Folger, T.A. (1988). *Fuzzy Sets, Uncertainty and Information*. Englewood Cliffs, N.J: Prentice Hall.
- Kosanovic, B.R. (1995). *Signal and System Analysis in Fuzzy Information Space*. University of Pittsburgh, PhD Thesis.

- Liau, L. Y. (2001). *Homeomorfisma Elipsoid dengan Sfera Melalui Struktur Permukaan Riemann serta Deduksi Pembuktiannya bagi Homeomorfisma FTTM*. Universiti Teknologi Malaysia, Tesis Sarjana.
- Liau, L. Y. (2004). *Algebraic Structures of FTTM for Neuromagnetic Inverse Problem*. 1<sup>st</sup> Year PhD Assessment, Universiti Teknologi Malaysia, Skudai, 18 Feb 2004.
- Lopes de Silva, F.H. and Van Rotterdam, A. (1987). Biophysical Aspects of EEG and MEG Meneration. In: Niedermeyer, E. and Lopes de Silva, F.H. *Electroencephalography: Basic Principles, Clinical Applications and Related Fields*. 2<sup>nd</sup> edition. Baltimore: Urban and Schwarzenberg, 15-28.
- Lueders, H., Lesser, R.P., Hahn, J., Dinner, D.S. and Klem, G. (1983). Cortical Somatosensory Evoked Potentials in Response to Hand Stimulation. *Journal of Neurosurgery*, 58: 885-894.
- Mosher, J. and Leahy, R. (1998). Recursive MUSIC: A Framework for EEG and MEG Source Localization. *IEEE Trans. Biomed. Eng.* 45: 1342-1354.
- Negnevitsky, M. (2002). *Artificial Intelligence: A Guide to Intelligent Systems*. England: Addison Wesley.
- Ooi T. H., Umi Kalthum Ngah, Noor Elaiza Khalid and Venkatachalam, P.A., (2000). *Region Growing Technique On Breast Ultrasound Images*. New Millenium International Conference On Pattern Recognition, Image Processing And Robot Vision, (PRIPOV 2000), Terengganu Advanced Technical Institute (TATI), Terengganu, 164-169.
- Paetau, R. (2002). Magnetoencephalography in Pediatric Neuroimaging, *Developmental Science*. 5(3): 361-370.
- Pal, S.K. (1992). *Fuzzy Sets in Image Processing and Recognition*. First IEEE International Conference on Fuzzy Systems, San Diego, CA. 119-126.

- Parker, J.R. (1994). *Practical Computer Vision*. Singapore: John Wiley.
- Penfield W. and Rasmussen, T. (1950). *The Cerebral Cortex of Man*. New York: Macmillan.
- Penfield, W. and Jasper, J. (1954). *Epilepsy and the Functional Anatomy of the Human Brain*. Boston MA: Little Brown and Co.
- Peters, M.J. (1997). *Volume Conduction effects in EEG and MEG*. University of Twente, The Netherlands, PhD Thesis.
- Phillips, J. W., Leahy, R.M. and Mosher, J.C. (1997). MEG-Based Imaging of Focal Neuronal Current Sources. *IEEE Trans. Med. Imaging*, 16: 338-348.
- Plonsey, R. (1981). Generation of Magnetic Fields by the Human Body (Theory). In: Erne, S.N., Hahlbohm, H.D. and Lubbig, H. *Biomagnetism*. Berlin : de Gruyter. 177-200.
- Pizella, V. and Romani, G. L. (1990). Principles of Magnetoencephalography. In: Sato S., *Magnetoencephalography. Advances in Neurology*. Volume 54, New York: Raven Press. 1-9.
- Rashdi Shah Ahmad, Tahir Ahmad and Chew S. L. (2001). Algorithm of Magnetic Flux Density on a Plane Generated by a Finite Length Current Source, *Jurnal Teknologi Maklumat dan Sains Kuantitatif*, 63-73.
- Ricardo, V., Sarela, J., Jousmaki, V., Hamalainen, M. and Oja, E. (2000). Independent Component Approach to the Analysis of EEG and MEG Recordings, *IEEE Transactions on Biomedical Engineering*, 47: 589-593.
- Risto, I., (1985). *Neuromagnetism: Theory, Techniques and Measurements*, Helsinki Univ of Technology, Thesis of Doctor of Technology.

- Risto, N., Risto, I. and Alho, K. (1994). Magnetoencephalography in Studies of Human Cognitive Brain Function. *Trends in Neurosciences*. 17: 389-398.
- Rose, D.F., Smith, P.D. and Sato, S. (1987). Magnetoencephalography and Epilepsy Research. *Science*. 238: 329-335.
- Ross, T.J. (2004). *Fuzzy Logic with Engineering Applications*, 2<sup>nd</sup> Edition. England: John Wiley.
- Sadiku, M. (1995). *Elements of Electromagnets*. New York: Oxford University Press.
- Sarvas, J. (1987). Basic Mathematical and Electromagnetic Concepts of the Biomagnetic Inverse Problem, *Physics in Medicine and Biology*. 32 (1): 11-22.
- Sato, S. (1990). *Advances in Neurology: Magnetoencephalography. Vol 54*: New York: Raven Press.
- Schmidt, R. (1986). Multiple Emitter Location and Signal Parameter Estimation. *IEEE Trans. Antennas Propag.* AP-34: 276-280.
- Schwartz, B.J. (1999). Magnetic Source Imaging as a Clinical Tool in Functional Brain Mapping. *GEC Review*. 14(2): 124-143..
- Sid-Ahmed, M.A. (1995). *Image Processing: Theory, Algorithms and Architectures*. Singapore: McGraw Hill.
- Tahir Ahmad, Rashdi Shah Ahmad, Fauziah Zakaria and Liau Li Yun (2000). Development of Detection Model for Neuromagnetic Fields. *Proceedings of the National Conference on Biomedical Engineering 2000*, Petaling Jaya, Selangor, Malaysia.

- Tahir Ahmad, Rashdi Shah Ahmad, Liao Li Yun, Fauziah Zakaria and Wan Eny Zarina Wan Abd Rahman (2004). Fuzzy Topographic Topological Mapping Version 2 (FTTM2) for Multiple Current Sources, *Simposium Sains Matematik 2004*, Johor, Malaysia.
- Tou, J. T. and Gonzalez, R.C. (1974). *Pattern Recognition Principles*. Reading, MA: Addison Wesley.
- Umi Kalthum Ngah, Ooi T. H., Venkatachalam, P.A. and Siti Noraini Sulaiman (2002). Mammographic Calcification Clusters Using The Region Growing Technique, *Proceedings of the 6<sup>th</sup> World Multiconference on Systemics, Cybernetics and Informatics*. SCI 2002, 14-18 July 2002, Orlando, Florida, USA, 147-152.
- Umi Kalthum Ngah, Nor Ashidi Mohd Isa and Masriah Mohd Nor (2003). Automated Seed-Based Region Growing Using the Moving K-Means Clustering for the Detection of Mammographic Microcalcifications” *CDROM Proceedings of the World Congress on Medical Physics and Biomedical Engineering (WC2003)*, 24-29 August, Sydney, Australia.
- Venkatachalam, P.A., Umi Kalthum Ngah and Ahmad Fadzil Mohd Hani and Ali Yeon Md Shakaff (2002). Seed-Based Region Growing Technique in Breast Cancer Detection and Embedded Expert System. *Proceedings of the International Conference on Artificial Intelligence And Technology. ICAiET 2002*, 17-18 June 2002, Kota Kinabalu, Sabah, 464-469.
- Wan Eny Zarina Wan Abdul Rahman, Tahir Ahmad and Rashdi Shah Ahmad (2002). Simulating The Neuronal Current Sources in the Brain. *Proceedings of the Kuala Lumpur International Conference on Biomedical Engineering 2002*. June 5-8. Kuala Lumpur, Malaysia. UM, 19-22.

- Wan Eny Zarina Wan Abdul Rahman, Tahir Ahmad and Rashdi Shah Ahmad (2003a). Determining The Number of Current Sources of Magnetoencephalography by Using a Fuzzy Clustering Technique. *Proceedings of the International Conference on Robotics, Vision, Information and Signal Processing (ROVISPS)*. January 22-24. Penang, Malaysia: IEEE, 777-780.
- Wan Eny Zarina Wan Abdul Rahman, Tahir Ahmad and Rashdi Shah Ahmad (2003b). Penentuan Bilangan dan Orientasi bagi Arus Bertindih Model FTTM. *Prosiding Simposium Kebangsaan Sains Matematik Ke XI*, Disember 22-24. Sabah, Malaysia: UMS, 307-314.
- Wiksw, J.P. Jr., (1983). Cellular Action Currents. In: Williamson, S.J., Kaufman G.L., and Modena, I. *Biomagnetism: An Interdisciplinary Approach*. New York: Plenum Press. 173-207.
- William, M. M., Raman, B.P. and Rangaraj, M.R. (1992). Region-Based Contrast Enhancement of Mammograms. *IEEE Transactions on Medical Imaging*. 11(3): 392-406.
- Williamson, S. J. and Kaufman, L. (1981). Biomagnetism. *Journal of Magnetism and Magnetic Materials*. 22: 129-201.
- Windham, M. P. (1982). Cluster Validity for the Fuzzy c-Means Clustering Algorithm. *IEEE Trans. Pattern Anal. Machine Intell.* 4(4): 357-363.
- Xie, X. L. and Beni, G. (1991). A Validity Measure for Fuzzy Clustering. *IEEE Trans. Pattern Anal. Machine Intell.* 13(8): 841-847.
- Yao, W., Hall, L.O., Goldgof, D.B. and Muller, K.F. (2000). Finding Green Riverin SeaWiFS Satellite Images. *Proceedings of the International Conference of Pattern Recognition*. Barcelona. 2: 307-310

Yung, Y.L. and Hsiang Y.Y. (2002). Magnetoencephalography and its Usefulness in Epilepsy Surgery. *Chinese Journal of Radiology*. 27: 273-279.

Zadeh, L. A. (1965). *Fuzzy Sets*. *Information and Control*, 8: 338-359.

Zhang, M., Hall, L.O. and Goldgof, D.B. (2000). Knowledge Extraction and Refinement from Multi Feature Images through (Re-) Clustering. *Proceedings of ICIG 2000*, Tianjin, China, 459-462.

Zimmerman, J.E., Thiene, P. and Harding, J.T. (1970). Design and Operation of Stable rf-biased Superconducting Point-Contact Quantum Devices and a note on the Properties of Perfectly Clean Metal Contact. *Journal of Applied Physics*, 41: 1572-1580.

Zimmermann, H. J. (1991). *Fuzzy Set Theory and its Applications*. 2<sup>nd</sup> ed. Dordrecht: Kluwer Academic.